The 2025 World Congress on
Advances in Structural Engineering and Mechanics (ASEM25)
BEXCO, Busan, Korea, August 11-14, 2025

Numerical study of RC beams strengthened with CFRP under close-in blast loading

Phi-Long Tran[1)] and *Jin-Kook Kim [2)]

[1), 2)] *Department of Civil Engineering, Seoul National University of Science and Technology, 232 Gongneung-ro, Nowon-gu, Seoul 01811, Republic of Korea*
[1)] *jinkook.kim@seoultech.ac.kr*

ABSTRACT

Structures in service may be subject to blast loading, which can result in significant damage or even failure of critical structural elements. Understanding and mitigating such effects is crucial for ensuring structural resilience. This study conducts a comprehensive numerical analysis to evaluate the efficiency of carbon fiber reinforced polymer (CFRP) as a reinforcing solution for reinforced concrete (RC) beams under explosive loads. Finite element (FE) models were developed using LS-DYNA to analyze the structural response, failure mechanisms of RC beams under blast conditions. To verify the reliability of the FE models, numerical results were systematically compared with experimental data from existing literature. CFRP reinforcement significantly enhances the load-carrying capacity and energy absorption of RC beams while also reducing mid-span deflection. Given the strong correlation between test and numerical outcomes, the study further explores the impact of different CFRP reinforcement strategies through numerical analyses, considering key factors such as CFRP thickness, the number of reinforcement layers, and various strengthening configurations.

1. INTRODUCTION

Recent terrorist bombing attacks and explosive accidents involving combustible materials have resulted in significant losses to property and human life. Reinforced concrete (RC) structures, widely used in civil infrastructure, have become main targets in such incidents (Tran et al., 2024). Notably, most of these explosions occurs inside or in close proximity to the affected building, highlighting the necessity of understanding of failure mechanisms and structural responses of RC components subjected to close-in blast loading for accurate damage assessment and effective anti-blast design.

The RC beam is one of the most fundamental components, playing a critical role in load transmission and structural connectivity. Under close-in explosions, RC beams are particularly vulnerable to various failure modes, including crushing damage on the front (blast-facing) side, localized spalling on the rear side, and punching shear failures (Almustafa et al., 2023). To assess the responses of RC beams, many experimental

---

[1)] Ph.D. Student
[2)] Associate Professor

studies have been carried out in the past few years. Zhang et al. (2013) conducted small-scale test on RC beam subjected to close-in explosive load and observed that the rapid arrival of the shockwave exerts high compressive pressure on the front surface of the RC beam. As the pressure wave propagates through the depth of beam and reaches the bottom surface, it reflects and induces tensile forces, causing cracking or spalling at the bottom side. These dynamic responses underline the significant role of concrete strength and stirrup reinforcement configuration in mitigating blast-induced damage. In related study, Rao et al. (2018) reported that the dominant failure mechanism of RC beams exposed to blast loads was a combination of bending and shear, especially at low scaled distances.

Although experiments are the most reliable method for assessing the behavior of RC structures under explosions, it is often unfeasible to perform comprehensive tests due to the wide variety of structure dimensions, material properties, and reinforcement configuration. Additionally, such tests are time-consuming and constrained by safety regulations. In contrast, numerical modelling provides an efficient and reliable alternative for rapidly assessing the blast response of RC components. Yang et al. (2022) conducted numerical simulations to examine the influence of beam depth on the extent of the damage zone in RC beams subjected to contact explosions. The results demonstrated a decreasing trend in damage span with increasing beam depth. Lin et al. (2019) conducted extensive numerical simulations and concluded that the damage severity increases with decreasing scaled distance, and this damage is strongly influenced by concrete strength, beam dimensions and reinforcement ratios. Their study also reviewed advanced numerical methods for simulating complex concrete failure mechanisms, including meshfree, and crack tracking approaches.

Carbon fiber reinforced polymers (CFRP) are commonly applied to enhance the blast resistance of conventional RC structures. In recent decades, extensive researches have been carried out to evaluate the blast resistance of RC components reinforced with CFRP materials, consistently demonstrating their effectiveness. Reifarth et al. (2021) validated the performance of external CFRP retrofitting on RC slabs exposed to blast loads, revealing that the reinforcement consistently reduced damage and proved to be cost-effective and easy to apply, making it a promising solution for enhancing blast resistance. Hu et al. (2021) conducted research experimentally and numerically and found that CFRP retrofitting effectively enhance the resistance to blast load of RC columns. CFRP wrapping prevents inelastic deformation and shifts failure from compression-shear to flexural modes, while the unwrapped end regions are critically weak points that control residual capacity, contrary to the usual mid-span failure in non-retrofitted columns.

Given the limited number of studies focusing on RC beams retrofitted with CFRP under blast loading, this research aims to address this gap through numerical investigation. Specially, the blast behavior of CFRP-strengthened RC beams is simulated using LS-DYNA, with the finite element model validated against experimental results reported by Yan et al. (2020). By conducting a direct comparison between retrofitted and non-retrofitted RC beams under identical blast conditions, the effectiveness of CFRP strengthening is quantitatively evaluated. Furthermore, a comprehensive parametric study is conducted to assess the influence of critical design parameters, such as CFRP thickness, width-to-depth (W/D) ratio, and bond strength

between concrete and CFRP, on blast resistance. Through this approach, the study provides insights into optimal retrofit configurations and enhances the understanding of the structural behavior of CFRP-strengthened RC beams under extreme dynamic loads, thereby contributing to the current knowledge base and bridging the research gap.

2. TEST OVERVIEW AND FEM MODEL ESTABLISHMENT

2.1 Information of test setup

Three RC columns, both retrofitted with CFRP and non-retrofitted, tested under close-in blast loading as reported by Yan et al. (2020), were selected to develop and validate the FEM models. The dimensions of three selected columns are illustrated in Fig. 1. All specimens feature a square cross-section of 150 x 150 mm and a length of 1700 mm. Four 12 mm diameter steel bars are utilized for longitudinal bars in each column, and 6 mm stirrups are placed at 180 mm spacing. The difference among these specimens lies in their CFRP retrofitting configuration. One specimen (F1-0) is non-retrofitted, another (F1-1) is strengthened with a 2 mm-thick CFRP sheet applied only to the bottom surface, and the third (F1-3) is retrofitted with 2 mm-thick CFRP layers applied both front and rear surfaces facing the explosion, as shown in Fig. 2.

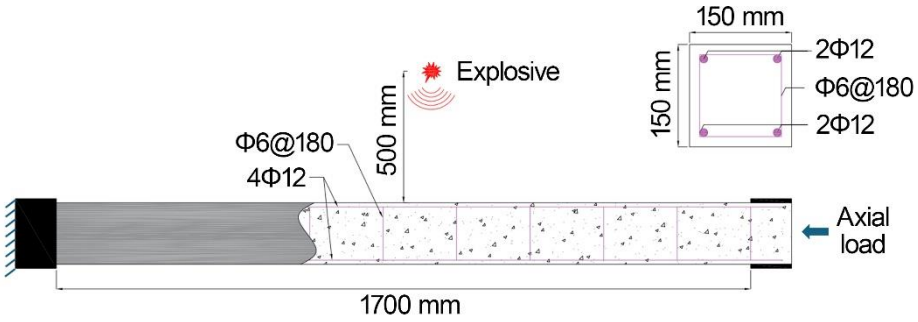

Fig. 1 Design details of specimen

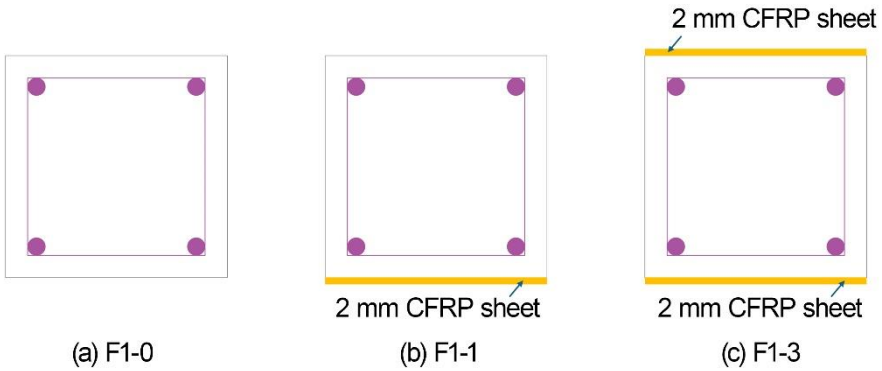

Fig. 2 CFRP retrofitted configuration

The concrete uniaxial compressive cylinder strength used in the tests is 31 MPa.

The longitudinal and lateral reinforcing steels exhibit yield stresses of 408 MPa and 544 MPa, respectively. Woven carbon fiber sheets were utilized for CFRP strengthening, with a tensile strength of 3140 MPa. The typical characteristics of utilized materials are tabulated in Table 1.

Table 1. Typical characteristics of the used materials (Yan et al., 2020)

Material	Yield strength (MPa)	Ultimate strength (MPa)	Elastic modulus (GPa)
Concrete		31	30
Longitudinal rebar	408	518	200
Transverse rebar	544	591	200
CFRP		3140	260

For the boundary conditions, as shown in Fig. 1, RC columns were fixed into a groove-shaped concrete foundation to ensure solid support. Axial prestress was applied to the columns to simulate static axial loading, utilizing hydraulic jacks and two strands, as illustrated in Fig. 3. The strands were anchored to steel plates positioned at both ends of the column. RC columns subject to transverse shock-wave loads, detonated by a 0.8 kg TNT explosive suspended above the column center at 0.5 m stand-off distance.

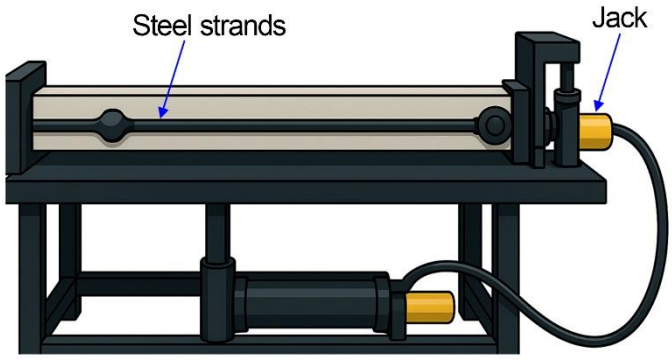

Fig. 3 Experiment setup

2.2 FEM model

LS-DYNA was utilized to develop FEM models, simulating the failure and damage behavior of the columns subjected to explosions. The 3D model is shown in Fig. 4.

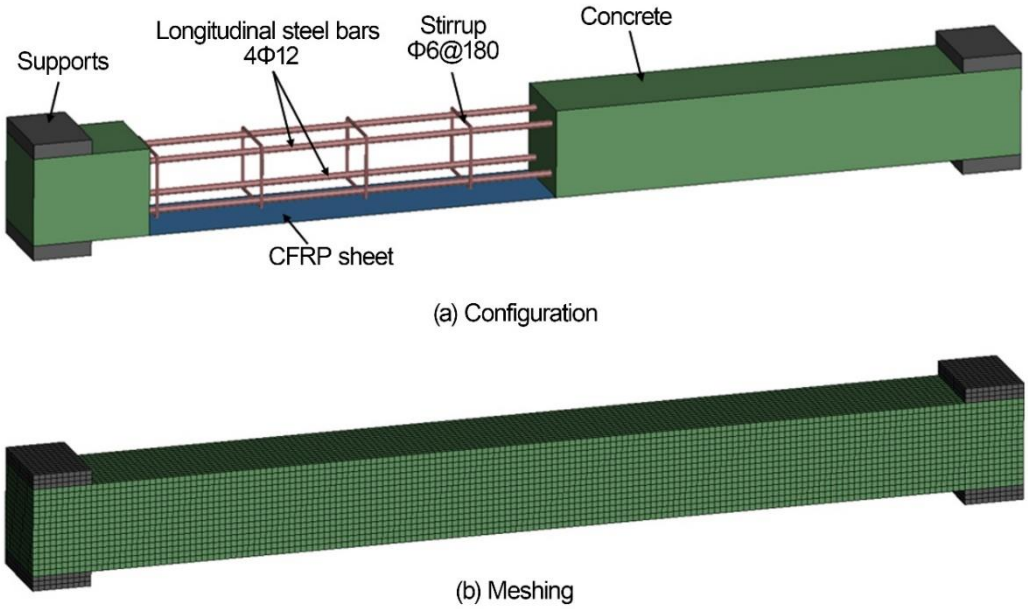

Fig. 4 FEM model development

In the FEM model, concrete elements were represented by 8-node solid hexahedral elements (SECTION_SOLID) with a mesh size of 10 x 10 x 10 mm. Transverse and longitudinal reinforcements were modeled using one-dimensional elements, type beam (SECTION_BEAM) with an element length of 10 mm. The CFRP layer was simulated using shell elements with a 10 mm grid size. A 10 mm mesh size was determined to be optimal through convergence analysis, considering both accuracy and simulation time.

The constitution models utilized in the FEM simulation are summarized in Table 2. Concrete was modeled with the Kargozian and Case model (K&C) (Park et al., 2024). The model is based on plasticity theory, featuring three shear failure surfaces and accounting for strain rate sensitivity. This material model allows for automatic parameter generation by merely inputting the unconfined compressive strength of concrete (Yoo and Yoon, 2016). Steel reinforcement was simulated using built-in material (Material model 24)(Zhang et al., 2025), which accurately captures the stress-strain relationship of steel rebars. Material type 54 was employed to model the CFRP sheets (Li et al., 2024), incorporating a failure criterion that considers nonlinear shear stress-strain behavior and post stress degradation (Zhang et al., 2022).

To account for the effect of high strain rates on the strength of concrete and steel reinforcements under blast loading, dynamic increase factor (*DIF*) models were utilized. These *DIF* values were determined by the empirical relationships introduced in the CEB-FIP model code, (1993) and modification models suggested by Malvar and Crawford (1998), as illustrated in Fig. 5.

Table 2. Material models used in LS-DYNA

Material	LS-DYNA model
Concrete	Mat_072R3 (*Mat_Concrete_Damage_Rel3)
Reinforcement bars	Mat_024 (*Mat_Piecewise_Linear_Plasticity)

CFRP Mat_054 (*Mat_Enhanced_Composite_Damage)

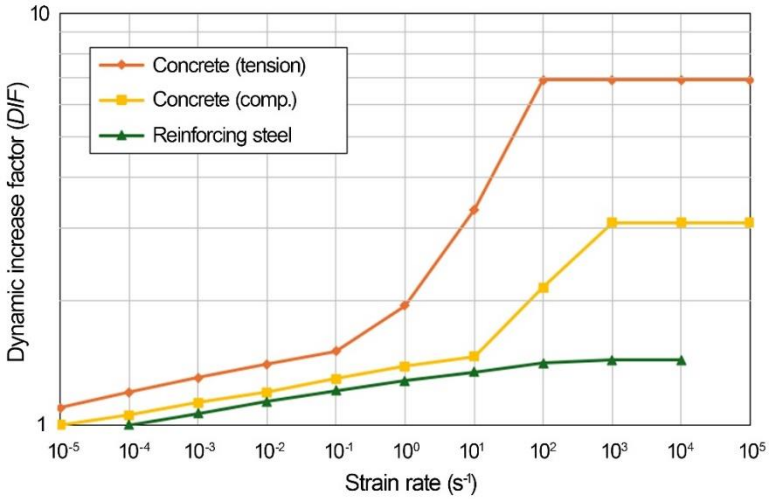

Fig. 5 Dynamic increase factor of concrete and steel materials

To facilitate the force transfer and deformations between concrete and steel rebars, the Constrained Beam in Solid keyword was employed, ensuring a fully bonded interaction between the two materials (Zhou et al., 2023). For the interface between the CFRP sheet and concrete, the contact algorithm in LS-DYNA (Automatic Surface To Surface Tiebreak) was adopted. This contact option enables simulation of adhesive bonding and allows for debonding behavior once predefined failure criterion, described by Eq. 1, is met (Alkhatib et al., 2020).

$$\left(\frac{|\sigma_n|}{NFLS}\right)^2 + \left(\frac{|\sigma_s|}{SFLS}\right)^2 \geq 1 \tag{1}$$

where, σ_n denotes the normal stress, while σ_s indicates shear stresses at the interface, respectively. The failure stresses *SFLS* and *NFLS* correspond to the shear and tensile failure strengths of the epoxy adhesive. The values of *NFLS* and *SFLS* were both taken as 15 MPa, based on the data reported the study of Mutalib and Hao (2011).

The blast loading was simulated in LS-DYNA using the Load Blast Enhanced keyword. The pressure magnitude was determined using the scaled distance formula $Z = R/W^{1/3}$, where R is the standoff distance and W is charge weight of equivalent TNT. In this study, the values of R and W were set to 0.5 m and 0.8 kg, respectively, consistent with the reference test setup. Additionally, an axial force was exerted to the top of the column using the Load Segment Set keyword. During the blast phase, the experimental results show excessive vertical displacement at mid-span, which leads to horizontal shortening of the column and, consequently, a reduction in its effective length. As a result, the axial prestress may be significantly diminished and completely lost. To reflect this behavior, the FEM model maintained the axial load for several milliseconds prior to the blast to allow the structure to reach static equilibrium. It was

then gradually reduced to zero at the point of blast-induced maximum deflection, consistent with the test conditions.

2.3 Model verification

Numerical results were validated against the corresponding experimental data from the reference study, which included three specimens as outlined in Fig. 2. The non-retrofitted column (F1-0) experienced high damage, characterized by the crushing and spallation at mid-span, indicating a flexural failure mode, as illustrated in Fig. 6. In contrast, the CFRP-retrofitted columns demonstrate enhanced resistance to blast loading, resulting in significantly smaller overall deflections. As illustrates in Fig. 6, the FEM calculation closely align with the experimental counterpart.

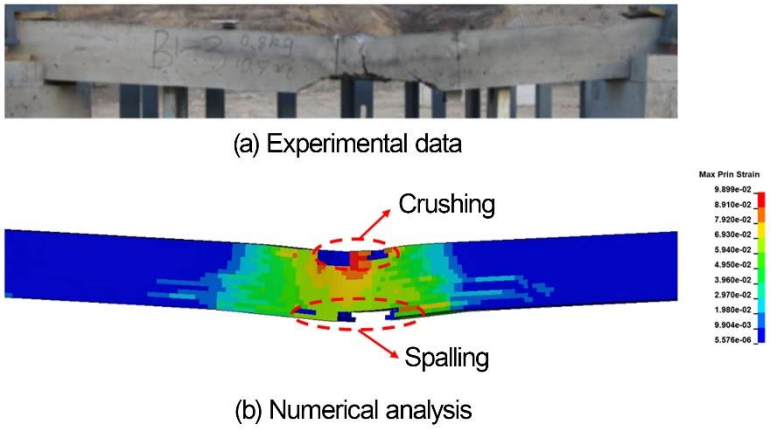

Fig. 6 Blast loaded RC column (F1-0)

The mid-span deflection versus time curves obtained from both the test and the FEM analyses are presented in Fig. 7 and summarized in Table 3. The peak mid-span displacements (δ) also show good agreement with the test data.

These comparisons indicate that the developed FEM models can reliably predict the damage mode, deformation and overall behavior of RC beams and columns under blast loading. The validated method is subsequently employed to perform comprehensive parametric study in the following section.

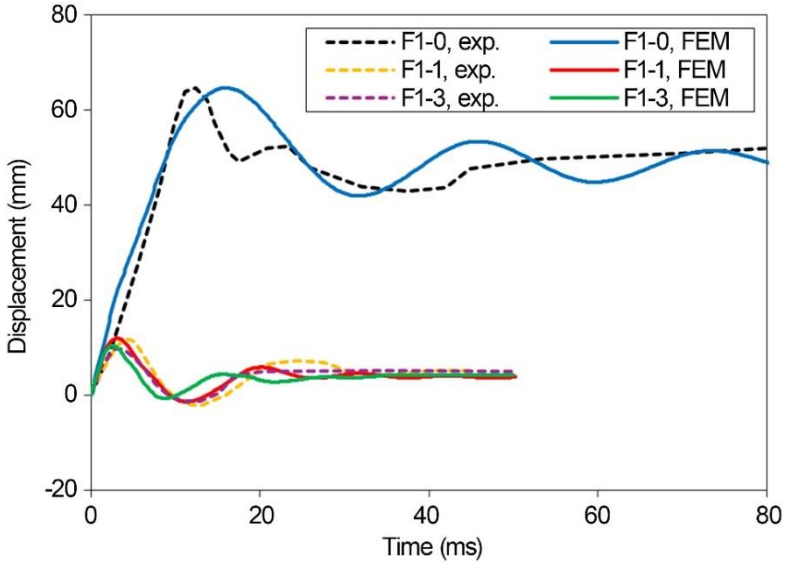

Fig. 7 Mid-span deflection time history

Table 3. Comparison of mid-span displacement

Specimen	Damage mode	δ_{exp} (MPa)	δ_{FEM} (GPa)	Error (%)
F1-0	Flexural	64.5	64.71	0.3
F1-1	Flexural	11.1	12.02	7.7
F1-3	Flexural	9.2	10.5	12.3

3. PARAMETRIC STUDY

Comprehensive numerical analyses were conducted to simulate the responses of RC beams strengthened with CFRP, considering various influencing parameters related to strengthening schemes. To ensure the practical relevance of analysis, the length of beams was set to 5000 mm, with a cross section of 350 mm x 500 mm. Longitudinal reinforcing bars consist of 3Φ25 mm compression zone and 3Φ25 mm for tension zone. The diameter of the transverse reinforcing bars is 10 mm, placed at 125 mm spacing, in accordance with CSA S850 (2012). To examine the dynamic responses of RC beams under blast load, the axial load was not applied in numerical analyses. The material characteristics of steel, concrete and CFRP were adopted consistently with those used in the validated FEM models.

3.1 Effect of CFRP thickness

Effect of CFRP thickness on the blast resistance was investigated by applying the varying thickness of 1 mm, 2 mm, 3 mm, 4 mm, and non-retrofitted case (0 mm). To simulate close-in blast loading, the explosive was placed at a distance of 1000 mm directly above the center of the beam. The explosive mass was varied, resulting in a range of scaled distance from 0.37 m/kg$^{1/3}$ to 0.69 m/kg$^{1/3}$. The analysis results are presented in Fig. 8.

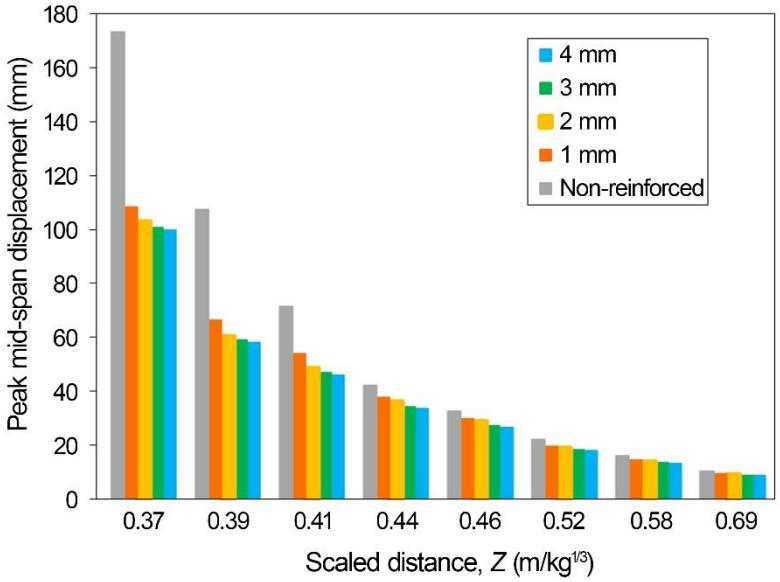

Fig. 8 Peak deflection at different Z

Overall, the displacement response of RC beams decreases with increasing CFRP thickness. Notably, the difference in response between retrofitted and non-retrofitted beams is significant. Taking the case of Z = 0.41 m/kg$^{1/3}$, the peak deflection reduces from 71.48 mm for non-retrofitted case (0 mm) to 53.78 mm, 48.31 mm, 46.72 mm and 45.78 mm for CFRP thicknesses of 1 mm to 4 mm, respectively. This trend remains consistent across all scaled distances.

When RC beams are subjected to low-intensity blast load (with Z larger than 0.58 m/kg$^{1/3}$), the enhancement in blast resistance due to increased CFRP thickness is not clearly observed. This is because, under such loading conditions, both concrete and steel reinforcement remain within the elastic range, thereby minimizing the contribution of CFRP strengthening, particularly with increased CFRP thickness. As illustrated in Fig. 9, the stress time history of the longitudinal reinforcing bars for two blast cases, low (Z = 0.69 m/kg$^{1/3}$) and high (Z = 0.46 m/kg$^{1/3}$), demonstrate this behavior. Furthermore, the internal energy absorbed by the concrete material under these two blast loading conditions, shown in Fig. 10, indicates that for the low blast load, RC beams retrofitted with different CFRP thicknesses exhibit relatively similar energy absorption. In contrast, under high blast loads, beams with thinner CFRP layers absorb significantly more energy in the concrete, leading to more severe damage and greater deflection.

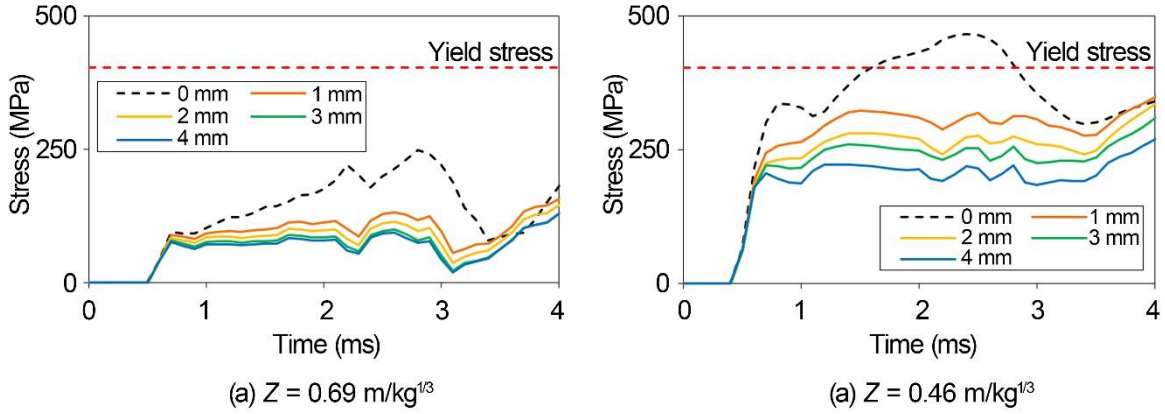

Fig. 9 Stress histories of longitudinal bars

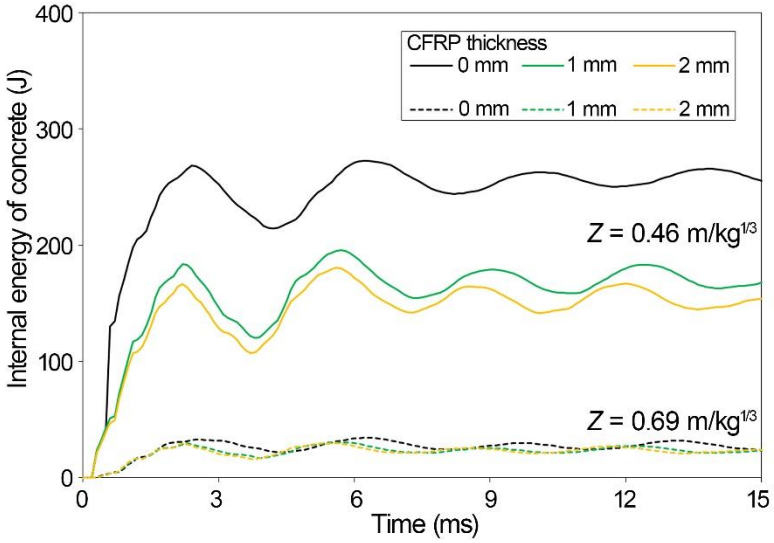

Fig. 10 Concrete internal energy

3.2 Effect of W/D ratio

The width-to-depth (*W*/*D*) ratio of RC beams plays a critical role in determining their blast resistance and the effectiveness of CFRP strengthening. In this study, various *W*/*D* ratios are investigated, while the moment of inertia ($I = W \times D^3/12$) is kept constant to ensure comparable flexural stiffness among the beams. Flexural reinforcement is accordingly designed to provide uniform flexural capacity across all specimens. Table 4 summarizes the geometric configurations and reinforcement details of the RC beams.

Table 4. Geometry and reinforcement configurations of RC beams

W/*D*	*W* (mm)	*D* (mm)	Flexural rebar	Flexural rebar ratio (%)
0.33	200	600	2Φ25	0.85
0.5	270	540	2Φ29	0.885

0.7	350	500	3Φ25	0.874
1.0	460	460	2Φ29 + 1Φ22	0.851

The RC beams were subjected to a blast load generated by a 15 kg explosive placed 1000 mm from mid-span. This analysis also considers varying CFRP thicknesses ranging from 1 mm to 4 mm. As illustrated in Fig. 11 (a), beams with lower width-to-depth (*W*/*D*) ratios exhibit greater flexural capacity, evidenced by reduced peak mid-span displacements.

To evaluate the efficiency of CFRP strengthening, the rate of change in peak displacement is assessed using the slope of the linear fit of maximum deflection across different CFRP thicknesses, as shown in Fig. 11 (b). The results indicate that beams with higher *W*/*D* ratios benefit more from CFRP strengthening, as reflected by the steeper slope. Conversely, beams with lower *W*/*D* ratios inherently possess higher flexural capacity, making CFRP reinforcement, especially with increased thickness, less effective, as the resulting improvement in capacity is marginal.

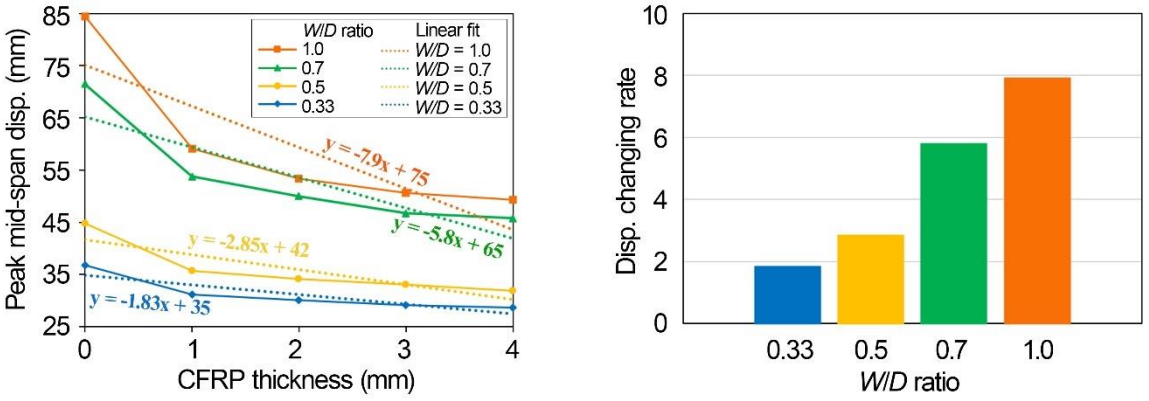

(a) Displacement vs. CFRP thickness across *W*/*D* Ratios (b) Effective of CFRP strengthening

Fig. 10 Displacement of RC beams with different *W*/*D* ratio

3.4 Effect of bond strength

The degree of composite action achieved between concrete and CFRP is primarily governed by interfacial bond strength. This study investigates the influence of varying bond strengths on the blast response of CFRP-retrofitted RC beams. In the analysis, the RC beams are strengthened with a 2 mm thick CFRP sheet fully covering the bottom surface. The bond strengths considered include 2.5 MPa, 5 MPa, 7.5 MPa, 10 MPa, 12 MPa, and 15 MPa, which are typical for practical applications (Kaur et al., 2024; Li et al., 2022). Blast loads are applied at different scaled distances of 0.41, 0.46, and 0.58 m/kg$^{1/3}$.

Fig. 12 presents the displacement responses of CFRP-retrofitted RC beams with various bond strengths. The results indicate that increase the bond strength enhances the blast resistance, evidenced by a reduction in peak mid-span deflection. However, this enhancement is only significant when the bond strength is below 7.5 MPa, further increases do not result in additional reductions in deflection. At this point, the failure

mode transitions from debonding at the interface to tensile rupture within the concrete itself. Therefore, any further increase in bond strength beyond this threshold has a negligible effect on the blast resistance of CFRP-retrofitted RC beams.

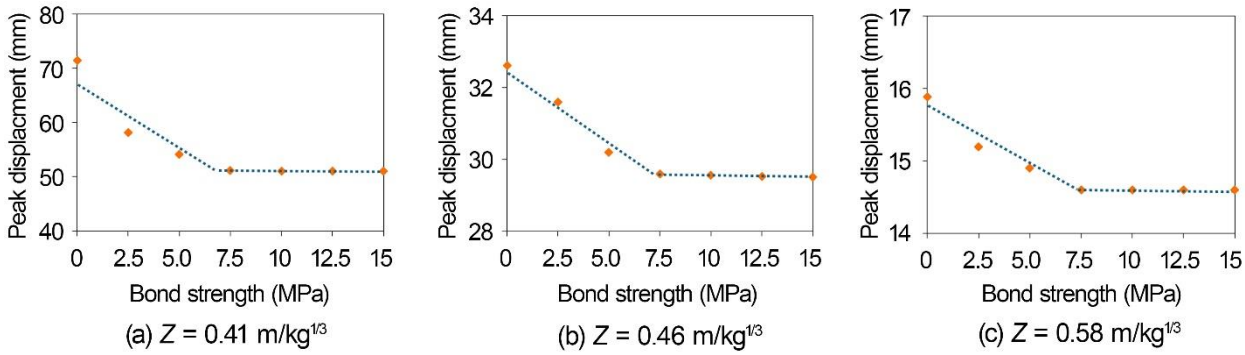

Fig. 12 Displacement of RC beams with different bond strength

3.4 Effect of CFRP retrofitting configuration

In this section, the effect of CFRP width (W_{CFRP}) applied to the rear surface of RC beams is examined. The CFRP is bonded along the full length of the beam at the center line, with the W_{CFRP} varied from 0.25W to 1.0W, where W is the beam width, as shown in Fig. 13 (a). The RC beams have dimensions of 350 mm (width) × 500 mm (depth) × 5000 mm (length) and are subjected to a 15 kg TNT equivalent explosive positioned 1000 mm away from the mid-span. The analysis results are presented in Fig. 13 (b).

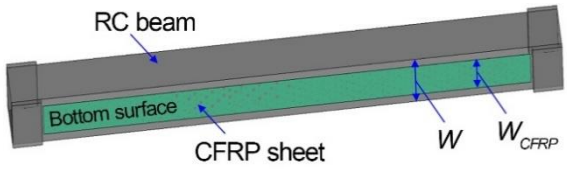

(a) CFRP-strengthed configuration

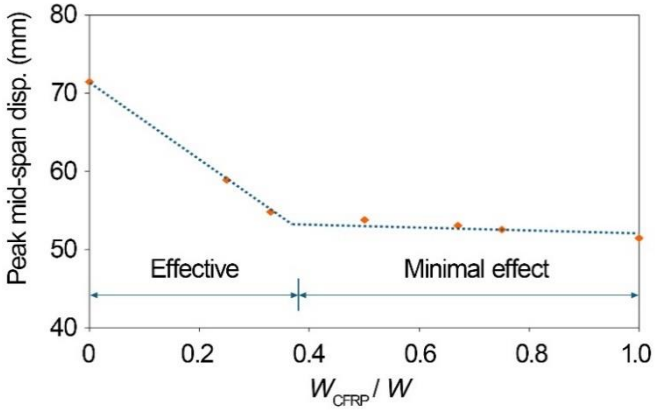

(b) Displacement of RC beams with different W_{CFRP}

Fig. 13 Displacement of RC beams with different W_{CFRP}

The results show that a significant reduction in peak mid-span displacement occurs when the ratio W_{CFRP}/W increases up to 0.4, demonstrating the effectiveness of the strengthening. Beyond this threshold, further increases in W_{CFRP} yield marginal increase in structural performance.

Fig. 14 presents the numerical deformation behavior of an RC beam under blast loading. The flexural strain exhibits a distinct non-uniform pattern across the beam width, with the peak plastic strain concentrated within the central 160 mm region, approximately 50% of the total beam width. In this zone, the effective plastic strain becomes significantly elevated, while it gradually diminishes toward the beam edges. Consequently, the CFRP layer installed at the center of the soffit is responsible for resisting the majority of tensile demand. When the CFRP width-to-beam width ratio (W_{CFRP}/W) is $\leq$ 0.4, the CFRP effectively covers the high-strain region, resulting in flexural stiffness increase corresponding reduction in mid-span displacement by approximately up to 25% compared to the non-retrofitted case. Beyond this threshold (W_{CFRP}/W > 0.4), the marginal gain diminishes as the extended CFRP covers regions where strain is significantly lower, contributing less than 2% to the additional displacement decrease.

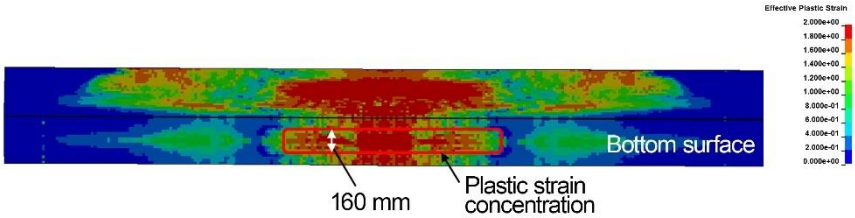

Fig. 14 Strain distribution in RC beam under explosion

4. CONCLUSIONS

3D FEM models were conducted to capture the dynamic response of RC beams retrofitted by CFRP sheet subjected to blast loading. The numerical models were compared with the experimental results, aimed at validating the reliability of the models. A comprehensive parametric study was performed in this research, providing conclusions as follows:

- CFRP reinforcement significantly improves the blast resistance of RC beams, with more pronounced effects under higher blast intensity. Increasing the CFRP thickness leads to a reduction in displacement.
- The *W*/*D* ratio of RC beams significantly influences their dynamic response to blast loading and the effectiveness of CFRP retrofitting. Beams with higher *W*/*D* ratios exhibit lower blast resistance compared to those with lower *W*/*D* ratios, resulting in greater peak displacements. In contrast, beams with lower *W*/*D* ratios inherently possess greater flexural capacity, thereby making the effect of CFRP reinforcement negligible.
- An increase in bond strength helps reduce the peak deflection of RC beams under blast loading. However, this effect converges at a bond strength of approximately 7.5 MPa; beyond this point, further increases in bond strength do not contribute to additional improvements in blast resistance provided by CFRP

retrofitting.

- A significant reduction in peak mid-span displacement is observed as the ratio of W_{CFRP} to beam width (W) increases up to 0.4. Beyond this threshold, further increases in W_{CFRP} result in only marginal improvements. Therefore, the CFRP reinforcement width can be optimized to balance structural performance with cost and construction convenience.

ACKNOWLEDGMENT

This study was supported by the Research Program funded by SeoulTech (Seoul National University of Science and Technology).

REFERENCES

Alkhatib, F., Mahdi, E., Dean, A., 2020. Crushing response of CFRP and KFRP composite corrugated tubes to quasi-static slipping axial loading: Experimental investigation and numerical simulation. Compos Struct 246, 112370. https://doi.org/10.1016/j.compstruct.2020.112370

Almustafa, M.K., Balomenos, G.P., Nehdi, M.L., 2023. Data-driven reliability framework for qualitative damage states of reinforced concrete beams under blast loading. Eng Struct 294, 116803. https://doi.org/10.1016/j.engstruct.2023.116803

Association, C.S., 2012. Design and assessment of buildings subjected to blast loads: CSA S850-12. Mississauga, ON: Canadian Standards Association 126.

Béton, C.E.-I. du, 1993. CEB-FIP model code 1990: Design code. Thomas Telford Publishing.

Hu, Y., Chen, L., Fang, Q., Kong, X., Shi, Y., Cui, J., 2021. Study of CFRP retrofitted RC column under close-in explosion. Eng Struct 227, 111431. https://doi.org/10.1016/j.engstruct.2020.111431

Kaur, M., Chawla, H., Kwatra, N., 2024. Bond performance of CFRP-concrete interface using different graphene derivative modified epoxies. Constr Build Mater 450, 138625. https://doi.org/10.1016/j.conbuildmat.2024.138625

Li, B., Hu, R., Bai, S., Dong, W., Zhao, Z., Song, L., 2022. Mechanical performance of concrete strengthened by modified epoxy resin bonded CFRP. J Adhes Sci Technol 36, 1764–1780. https://doi.org/10.1080/01694243.2021.1984086

Li, G., Wang, J., Li, X., Zhou, Y., Liu, R., 2024. Dynamic behavior of concrete filled steel tubular columns internally strengthened with I-shaped CFRP against vehicular bombs. Structures 69, 107598. https://doi.org/10.1016/j.istruc.2024.107598

Lin, S.-C., Li, D., Yang, B., 2019. Experimental study and numerical simulation on damage assessment of reinforced concrete beams. Int J Impact Eng 132, 103323. https://doi.org/10.1016/j.ijimpeng.2019.103323

Malvar, L.J., Crawford, J.E., 1998. Dynamic increase factors for concrete. DTIC document 1, 1–6.

Mutalib, A.A., Hao, H., 2011. Numerical Analysis of FRP-Composite-Strengthened RC Panels with Anchorages against Blast Loads. Journal of Performance of Constructed Facilities 25, 360–372. https://doi.org/10.1061/(ASCE)CF.1943-5509.0000199

Park, S., Kim, K., Kim, D., Park, Y.-J., Shim, B., 2024. Verification of Protection Performance of Concrete Blast-Proof Panels Against Internal Explosions. Int J Concr Struct Mater 18, 44. https://doi.org/10.1186/s40069-024-00662-3

Rao, B., Chen, L., Fang, Q., Hong, J., Liu, Z., Xiang, H., 2018. Dynamic responses of reinforced concrete beams under double-end-initiated close-in explosion. Defence Technology 14, 527–539. https://doi.org/10.1016/j.dt.2018.07.024

Reifarth, C., Castedo, R., Santos, A.P., Chiquito, M., López, L.M., Pérez-Caldentey, A., Martínez-Almajano, S., Alañon, A., 2021. Numerical and experimental study of externally reinforced RC slabs using FRPs subjected to close-in blast loads. Int J Impact Eng 156, 103939. https://doi.org/10.1016/j.ijimpeng.2021.103939

Tran, P.-L., Tran, V.-L., Kim, J.-K., 2024. Mid-span displacement and damage degree predictions of RC beams under blast loading using machine learning-based models. Structures 65, 106702. https://doi.org/10.1016/j.istruc.2024.106702

Yan, J., Liu, Y., Xu, Z., Li, Z., Huang, F., 2020. Experimental and numerical analysis of CFRP strengthened RC columns subjected to close-in blast loading. Int J Impact Eng 146, 103720. https://doi.org/10.1016/j.ijimpeng.2020.103720

Yang, C., Jia, X., Huang, Z., Zhao, L., Shang, W., 2022. Damage of full-scale reinforced concrete beams under contact explosion. Int J Impact Eng 163, 104180. https://doi.org/10.1016/j.ijimpeng.2022.104180

Yoo, D.-Y., Yoon, Y.-S., 2016. A Review on Structural Behavior, Design, and Application of Ultra-High-Performance Fiber-Reinforced Concrete. Int J Concr Struct Mater 10, 125–142. https://doi.org/10.1007/s40069-016-0143-x

Zhang, D., Yao, S., Lu, F., Chen, X., Lin, G., Wang, W., Lin, Y., 2013. Experimental study on scaling of RC beams under close-in blast loading. Eng Fail Anal 33, 497–504. https://doi.org/10.1016/j.engfailanal.2013.06.020

Zhang, R., Li, Hao-wen, Zhi, X., Li, F., Zhao, M., Li, Hang, 2025. Numerical simulation method and dent-model of circular steel tubes under low-speed impact. J Constr Steel Res 234, 109698. https://doi.org/10.1016/j.jcsr.2025.109698

Zhang, Y., Zhou, Y., Lu, Z., 2022. Evaluation of failure criteria for composite plate under high-velocity impact. Journal of Mechanical Science and Technology 36, 3291–3300. https://doi.org/10.1007/s12206-022-0609-5

Zhou, F., Cheng, Y., Peng, Q., Wu, H., 2023. Influence of steel reinforcement on the performance of an RC structure subjected to a high-velocity large-caliber projectile. Structures 54, 716–731. https://doi.org/10.1016/j.istruc.2023.05.096